

## Cetuximab Pharmacokinetics Influences Progression-Free Survival of Metastatic Colorectal Cancer Patients

Nicolas Azzopardi<sup>1,2</sup>, Thierry Lecomte<sup>1,2,3</sup>, David Ternant<sup>1,2,4</sup>, Michelle Boisdron-Celle<sup>6</sup>, Friedrich Piller<sup>7</sup>, Alain Morel<sup>6</sup>, Valérie Gouilleux-Gruart<sup>1,2,5</sup>, Céline Vignault-Desvignes<sup>1,2,4</sup>, Hervé Watier<sup>1,2,5</sup>, Erick Gamelin<sup>6</sup>, and Gilles Paintaud<sup>1,2,4</sup>

### Abstract

**Purpose:** An ancillary phase II study was conducted to study interindividual variability in cetuximab pharmacokinetics and its influence on progression-free survival (PFS) in metastatic colorectal cancer patients cotreated with irinotecan and 5-fluorouracil.

**Experimental Design:** Ninety-six patients received cetuximab as an infusion loading dose of 400 mg/m<sup>2</sup> followed by weekly infusions of 250 mg/m<sup>2</sup>. Doses of irinotecan and 5-fluorouracil were adjusted individually. Cetuximab concentrations were measured by ELISA. Compartmental pharmacokinetic parameters were estimated by a population approach, and PFS was analyzed using a Cox model.

**Results:** Cetuximab pharmacokinetics was best described using a two-compartment model with both first-order and saturable (zero-order) elimination. Estimated pharmacokinetic parameters (% standard error) were as follows: central volume of distribution  $V_1 = 2.96$  L (4%), peripheral volume of distribution  $V_2 = 4.65$  L (6%), elimination clearance  $CL = 0.497$  L/d (4%), distribution clearance  $Q = 0.836$  L/d (8%), and zero-order elimination rate  $k_0 = 8.71$  mg/d (10%). Body surface area influenced  $V_1$ ,  $V_2$ , and  $k_0$ . Pretreatment serum albumin influenced  $CL$ . Risk of disease progression decreased with cetuximab global clearance (cumulative dose/cumulative area under the concentration versus time curve;  $P = 0.00016$ ). Median PFS of patients with a cetuximab residual concentration on day 14 below median value was 3.3 months as compared with 7.8 months for the other patients ( $P = 0.004$ ).

**Conclusions:** Cetuximab pharmacokinetics in colorectal cancer patients can be described using a model combining linear and nonlinear elimination rates. PFS is influenced by global clearance of cetuximab, a parameter that can be estimated using cetuximab residual concentration on day 14. *Clin Cancer Res*; 17(19):6329–37. ©2011 AACR.

### Introduction

Colorectal cancer is one of the most common causes of cancer death in the Western world, ranking second in Europe and third in the United States (1). Cetuximab (Erbiximab), an IgG1 $\kappa$  monoclonal antibody binding to the extracellular domain of the epidermal growth factor receptor (EGFR), has shown relevant clinical activity in the

treatment of patients with chemotherapy-resistant metastatic colorectal cancer (2–4). Recently, data from an increasing number of studies have suggested that response to cetuximab seems confined to patients with metastatic colorectal cancer bearing tumors with wild-type *KRAS* (5–8), but the results are still inconclusive, partially because of the relatively small sample size of each study (9). Even in patients with wild-type *KRAS* tumor, an interindividual variability in response to cetuximab is observed. New prognostic and predictive factors are therefore needed to improve patient management.

Part of the interindividual variability in response to cetuximab may be explained by the interindividual variability in its pharmacokinetics. Fracasso and colleagues observed, in patients treated for different types of carcinomas, that responders had higher cetuximab trough serum concentrations than nonresponders (10). Interindividual pharmacokinetic variability has indeed been reported for all monoclonal antibodies (11, 12).

The aim of the present study was to analyze the influence of cetuximab pharmacokinetics on progression-free survival (PFS) of metastatic colorectal cancer patients treated with

**Authors' Affiliations:** <sup>1</sup>Université François Rabelais Tours; <sup>2</sup>CNRS, UMR 6239 (GICC), CHRU de Tours, Tours; Departments of <sup>3</sup>Hepato-Gastroenterology, <sup>4</sup>Pharmacology-Toxicology, and <sup>5</sup>Immunology, <sup>6</sup>INSERM U892 (CRCNA) Paul Papin Cancer Center, Cancer Biopathology Department, Angers; and <sup>7</sup>CNRS, Centre de Biophysique Moléculaire UPR 4301, Orléans, France

**Note:** Supplementary data for this article are available at Clinical Cancer Research Online (<http://clincancerres.aacrjournals.org/>).

**Corresponding Author:** Gilles Paintaud, Department of Pharmacology-Toxicology, Tours University Hospital, 2 Boulevard Tonnellé, 37044 Tours, Cedex 9, France. Phone: 33-247-476-007; Fax: 33-247-476-011; E-mail: [paintaud@med.univ-tours.fr](mailto:paintaud@med.univ-tours.fr)

**doi:** 10.1158/1078-0432.CCR-11-1081

©2011 American Association for Cancer Research.

### Translational Relevance

Cetuximab, a monoclonal antibody (mAb) binding to the extracellular domain of epidermal growth factor receptor (EGFR), is approved for use in combination with irinotecan and 5-fluorouracil chemotherapy in metastatic colorectal cancer. However, even in patients with wild-type *KRAS* tumor, an interindividual variability in response to cetuximab is observed. Our data are the first to show that cetuximab global clearance, that is, the individual capacity of disposition of this mAb from the body, influences progression-free survival (PFS). Cetuximab global clearance can be assessed early after treatment initiation by measuring residual cetuximab serum concentration on day 14. This concentration is also significantly related to PFS and could be used as a therapeutic drug monitoring tool to predict individual response of patients with metastatic colorectal cancer to treatment.

cetuximab in association with optimized 5-fluorouracil and irinotecan doses.

### Materials and Methods

#### Patients

This ancillary study was part of a multicenter, noncomparative, open-label, phase II study (ClinicalTrials.gov identifier: NCT00559741) that enrolled patients between October 2005 and January 2008. The study was designed in accordance with legal requirements and the Declaration of Helsinki and was approved by the ethics committee of Angers University Hospital, France. All patients gave written informed consent. Eligible patients (18–80 years old) had histologically confirmed stage IV colorectal adenocarcinoma with unresectable metastases, immunohistochemically detectable EGFR expression in the primary tumor or metastases, more than one unidimensionally measurable lesion outside previously irradiated areas, a life expectancy of 3 months or more, a Karnofsky performance status of more than 60, a WHO performance status of 2 or less, satisfactory hematologic checkup, and no complete dihydropyrimidine dehydrogenase (DPD) deficiency. Main exclusion criteria were symptomatic uncontrolled cerebral or meningeal metastases, concomitant radiotherapy, and any previous or current cancer (except skin cancer, *in situ* uterine cancer, or curatively treated breast cancer). The influence of *KRAS* status on response to cetuximab has been described after the initiation of this study (5). The analysis of *KRAS* mutation was therefore conducted retrospectively on resected tumors for patients who gave a specific, written informed consent.

#### Study design and treatment

The main study was designed to evaluate the safety and efficacy of irinotecan individual dose intensification. All

patients received cycles combining weekly cetuximab and every other week chemotherapy, consisting of irinotecan and 5-fluorouracil. Cetuximab was administered as a 2-hour infusion loading dose of 400 mg/m<sup>2</sup> followed by weekly 1-hour infusions of 250 mg/m<sup>2</sup>. Irinotecan dosing was adjusted according to *UGT1A1* genetic polymorphism. The standard 180 mg/m<sup>2</sup> dose was not modified in 6/7 [(TA)<sub>6</sub>TAA/(TA)<sub>7</sub>TAA] patients. After a first 180 mg/m<sup>2</sup> irinotecan dose, those of 5/5, 5/6, 5/7, and 6/6 patients were increased by 20% at each cycle, if tolerance was satisfactory, with a maximum dose of 300 mg/m<sup>2</sup>. The dose of 7/7 patients was reduced to 126 mg/m<sup>2</sup> (30% lower than standard 180 mg/m<sup>2</sup> dose). After a 200 mg/m<sup>2</sup> intravenous bolus of leucovorin, 5-fluorouracil was administered as a 400 mg/m<sup>2</sup> 10-minute intravenous push followed by a 46-hour infusion. The initial 5-fluorouracil dose was adjusted according to *DPD* genotype and phenotype as described previously (13). Then, the dose was tailored according to Paul Papin Cancer Center's practice, using pharmacokinetic monitoring as previously described (14) on the basis of 5-fluorouracil plasma concentrations measured after 43 hours (steady-state concentration). Dose-adjustment charts were based on previously reported ones (15) but adapted to bolus injection followed by 46-hour infusion. At the enrollment visit and every 3 months, an extensive checkup was done. At each visit, the weight was measured to adjust doses to body surface area (BSA).

#### *KRAS* and *FCGR3A* genotyping

***KRAS* mutation.** Formalin-fixed, paraffin-embedded (FFPE) tissues from 51 individuals harboring histologically confirmed metastatic colorectal cancer were analyzed retrospectively. Five FFPE sections per sample, mounted on glass slides, were reviewed for tumor content by an experienced pathologist. The indicated tumor cell areas were scraped with a scalpel. Genomic DNA was extracted with QIAamp DNA FFPE Tissue Kit (QIAGEN GmbH) according to the manufacturer's protocol. DNA concentration was determined by spectrofluorometric measurements. PCR was used to amplify part of the *KRAS* exon 2 and exon 3, and single-strand DNA preparation and pyrosequencing on a PSQ 96 pyrosequencer (Biotage) were done as previously described (16). After adding specific sequencing primers, samples were run and analyzed on a PSQ 96 pyrosequencer (Biotage).

***FCGR3A* genotyping.** After genomic DNA extraction from whole blood, *FCGR3A*-V158F genotyping was done by an allele-specific real-time PCR assay based on SYBR Green fluorescence (17).

#### Cetuximab pharmacokinetic analysis

Blood samples were collected to measure cetuximab serum concentrations. At the time of first infusion, blood samples were collected 2, 3.5, and 5.5 hours after the beginning of the infusion. Every other week, blood samples were collected before and 44 hours after the beginning of the infusion. Cetuximab serum concentrations were measured by a validated ELISA (18). Limit of detection was

0.012 mg/L and lower limit of quantitation (LLOQ) was 0.75 mg/L. Data were analyzed using the nonlinear mixed-effect modeling software MONOLIX 3.1 (19, 20), a population pharmacokinetic software. The use of MONOLIX Simulated Annealing function and 6 Markovian chains per run allow the algorithm to converge. A run was accepted only when the Fisher information matrix was obtained.

**Structural model design.** A dose dependency of cetuximab pharmacokinetics was previously reported (21–25). This phenomenon was also observed in the present study, with an accelerated decrease at low concentrations. One- and 2-compartment models with first-order and/or saturable elimination from the central compartment were tested to describe this nonlinearity. To describe the saturable component of the elimination of cetuximab, a Michaelis–Menten equation with maximum elimination rate ( $V_{\max}$ ) and the Michaelis–Menten constant ( $K_m$ ) was first tested. Although the fitting of the data was good,  $K_m$  could not be estimated reliably because it was below the LLOQ (0.75 mg/L). Therefore, the saturable component of the elimination was simplified to zero-order elimination, described by constant  $k_0$ . The other pharmacokinetic parameters were central ( $V_1$ , with concentration  $C_1$ ) and peripheral ( $V_2$ , with concentration  $C_2$ ) volumes of distribution and systemic (CL) and distribution (Q) clearances. The model is as follows:

$$\frac{dC_1}{dt} = -CL \cdot C_1 - Q \cdot C_1 + Q \cdot C_2 - k_0$$

$$\frac{dC_2}{dt} = +Q \cdot C_1 - Q \cdot C_2$$

The final model included random effects for all pharmacokinetic parameters. A proportional error model gave the best description of residuals. All models were compared using goodness-of-fit and residual plots, Akaike's information criteria, and other standard validation procedures.

**Covariates.** Before building the covariate model, all potential covariates were plotted against each other to identify any strong correlation to avoid simultaneous inclusion of correlated predictors (26). Several continuous covariates were tested: age, weight, BSA, irinotecan dose, initial serum albumin, and initial blood counts. Continuous covariates (COV) were centered on their median value  $COV_{\text{med}}$ , as follows

$$\theta_{\text{TV}} = \theta_0 \times \left( \frac{\text{COV}}{\text{COV}_{\text{med}}} \right)^{\beta_{\text{COV}}}$$

where  $\theta_0$  is the value of  $\theta$  for a median subject and  $\beta_{\text{COV}}$  quantifies the influence of COV on  $\theta$ .

The influence of following discrete covariates was tested: sex, initial disease grade (1–4), *DPD* activity (normal or deficient), *UGT1A1* polymorphisms (6/6 vs. 6/7 or 7/7), and line of treatment (first or second). Discrete covariates (CAT) on  $\theta_{\text{TV}}$  were implemented as follows:

$$\ln(\theta_{\text{TV}}) = \ln(\theta_{\text{CAT=ref}}) + \sum_{i=1}^n \beta_{\text{CAT}=i}$$

where  $\theta_{\text{CAT=ref}}$  is the value of  $\theta_{\text{TV}}$  for an arbitrary reference category, and  $\beta_{\text{CAT}=i}$  leads to the value of  $\theta_{\text{TV}}$  for the  $i$ th category.

The covariate model was built using a stepwise forward addition/backward deletion modeling approach (27). Inclusion of a covariate–parameter relationship was based on the likelihood ratio test. A covariate was included in the model during a forward addition step if a significant ( $P < 0.05$ ) decrease in the objective function value was observed (e.g., of 3.84 for 1 *df*). A covariate was kept in the model during a backward deletion step if a significant ( $P < 0.001$ ) increase in the objective function value was observed (e.g., 10.83 for 1 *df*).

**Secondary parameters.** Because only time-independent prognostic factors can be included in a Cox model and because our pharmacokinetic model combines concentration-dependent and concentration-independent elimination rates, we used a global nonparametric pharmacokinetic parameter to quantify cetuximab elimination. Cumulative area under the cetuximab concentration versus time curve (cumulative AUC) at the time of the event (progression, death, or censoring) was computed during the estimation of the model parameters. Cetuximab global clearance at the time of the event was calculated by dividing cumulative cetuximab dose by cumulative AUC. Because the assessment of cetuximab global clearance requires pharmacokinetic modeling using samples taken over time, we investigated whether early cetuximab residual concentration (day 14) could provide an index of patient exposure, using only data from patients who received the first 2 scheduled cetuximab injections (71 patients).

### PFS analysis

Time to progression was calculated as the delay between the first day of cetuximab treatment and the first observation of disease progression or death from any cause. If a patient had not progressed or died, time to progression was censored at the time of last known follow-up visit. Median PFS and its 95% CI were estimated by the Kaplan–Meier method. The hazard ratios (HR) were estimated by univariate and multivariate Cox proportional hazards regression models. The influence of potential prognostic factors on HRs was tested by likelihood ratio with and without the prognostic factor. Different time-independent potential prognostic factors were tested, both continuous (age, irinotecan mean weekly dose, cetuximab systemic clearance, zero-order elimination constant  $k_0$ , and cetuximab global clearance, i.e., cumulative dose divided by cumulative AUC) and categorical (sex, first or second line, cetuximab global clearance below or above median value, *KRAS* status, *FCGR3A-V158F*, *UGT1A1* genotypes, and cetuximab-related skin toxicity as described later).

### Cetuximab-related skin toxicity

Toxicity was graded for severity from grades 1 to 5 according to the Common Terminology Criteria for Adverse Events (CTCAE) v3.0 scale. Treatment had to be stopped in

case of grade 4 severity and the French drug agency (Afssaps) had to be notified. Cetuximab-related skin toxicity was reported as the higher grade of dermatologic adverse events, with the exclusion of hand-foot skin reaction that is mainly due to 5-fluorouracil (28). Cetuximab-related skin toxicity was analyzed on days 7, 14, and 21.

## Results

Ninety-six patients were included (Table 1). A total of 1,253 cetuximab serum concentrations (mean of 13 samples per patient) were available. Median residual concentrations were 41 and 54 mg/L on days 14 and 28, respectively. Except for pretreatment samples, only 28 concentrations were below LLOQ (0.75 mg/L; ref. 18) and were

left-censored. Therefore, the estimation of maximum likelihood was unbiased (29). A 2-compartment model with both first- and zero-order eliminations gave the best results. This model could indeed describe both high and low concentrations of cetuximab (Fig. 1). Saturable elimination was most important at concentrations below 10 mg/L, whereas linear elimination was preponderant at high concentrations. Volumes of distribution of the central ( $V_1$ ) and the peripheral ( $V_2$ ) compartments as well as saturated elimination rate ( $k_0$ ) increased with BSA. Inclusion of BSA reduced the variances of  $V_1$ ,  $V_2$ , and  $k_0$  by 15%, 17%, and 12%, respectively (Table 2). Initial serum albumin concentration was significantly related to first-order elimination clearance of cetuximab; this parameter decreases when serum albumin increases. Inclusion of initial serum albumin reduced  $CL$  variance by 8.3%. Other tested covariates did not influence cetuximab pharmacokinetics.

Within the first 7 days of treatment, patients who had had higher cetuximab-related skin toxicity grade equal or superior to 2 had a higher  $k_0$  value ( $P = 0.014$ ). The same relation was observed for the first 14 days of treatment ( $P = 0.036$ ). No significant relationship was observed between cetuximab-related skin toxicity and cetuximab  $CL$  or global clearance.

Median PFS of the overall group of 96 patients was 6.5 months (95% CI: 5.4–7.4; Table 3). Cetuximab global clearance had a significant influence on PFS, with risk of disease progression decreasing with cetuximab global clearance ( $P = 0.00016$ ). Median PFS of patients with a cetuximab global clearance below median value was 8.5 months as compared with 3.3 months for the other patients ( $P = 0.000049$ ; Fig. 2A). Residual cetuximab concentrations measured on day 14 were log-linearly related with global clearance ( $r^2 = 0.54$ ; Fig. 3). Median PFS of patients with a cetuximab residual concentration on day 14 below median value was 3.3 months as compared with 7.8 months for the other patients ( $P = 0.004$ ).

In the subgroup of 51 patients with known *KRAS* tumor status, median PFS was 6.6 and 7.1 months in patients with wild-type *KRAS* and mutated *KRAS* tumor, respectively ( $P = 0.66$ ). The influence of cetuximab global clearance on risk of disease progression was confirmed in the subgroup of patients with wild-type *KRAS* tumor: median PFS of patients with cetuximab global clearance below median value was significantly longer than that of the other patients (9.2 vs. 3.1 months, respectively,  $P = 0.013$ ; Fig. 2B). In the wild-type *KRAS* group, median PFS of patients with a cetuximab residual concentration on day 14 below median value was 3 months as compared with 10 months for the other patients ( $P = 0.03$ ).

No influence of cetuximab global clearance on median PFS was observed in the mutated *KRAS* group. No significant influence of *FCGR3A* polymorphism on PFS was observed in the whole population. In wild-type *KRAS* patients, a trend toward a better PFS was observed in *FCGR3A*-158V/V patients, with a time to progression of 10.1 months vs. 6.0 months for *FCGR3A*-158F allele carriers ( $P = 0.51$ ). Of note, 3 of 6 V/V patients discontinued

**Table 1.** Baseline characteristics of metastatic colorectal cancer patients ( $n = 96$ )

|                                   | Median   | Range     |
|-----------------------------------|----------|-----------|
| Age, y                            | 63       | 38–80     |
| Body weight, kg                   | 73       | 34–113    |
| BSA, m <sup>2</sup>               | 1.79     | 1.21–2.27 |
| Initial albuminemia, g/L          | 38       | 25–49     |
|                                   | <b>n</b> | <b>%</b>  |
| Sex                               |          |           |
| Male                              | 53       | 55.2      |
| Female                            | 43       | 44.8      |
| Line                              |          |           |
| First                             | 17       | 17.7      |
| Second                            | 79       | 82.3      |
| Primary tumor site <sup>a</sup>   |          |           |
| Colon                             | 56       | 57.1      |
| Rectum                            | 26       | 26.5      |
| Hinge rectosigmoid                | 14       | 14.3      |
| Other                             | 2        | 2.0       |
| No. of measured lesions           |          |           |
| 1                                 | 17       | 17.7      |
| 2                                 | 25       | 26.0      |
| 3                                 | 19       | 19.8      |
| >3                                | 25       | 26.0      |
| WHO baseline performance status   |          |           |
| 0                                 | 60       | 62.5      |
| 1                                 | 29       | 30.2      |
| 2                                 | 7        | 7.3       |
| <i>FCGR3A</i> -V158F polymorphism |          |           |
| F/F                               | 32       | 33.3      |
| F/V                               | 47       | 49.0      |
| V/V                               | 17       | 17.7      |
| Tumor <i>KRAS</i> status          |          |           |
| Wild-type                         | 32       | 62.7      |
| Mutated                           | 19       | 37.3      |
| Nonassessable                     | 45       | –         |

Abbreviations: F, phenylalanine; V, valine.  
<sup>a</sup>Two patients had 2 different primary tumor sites.

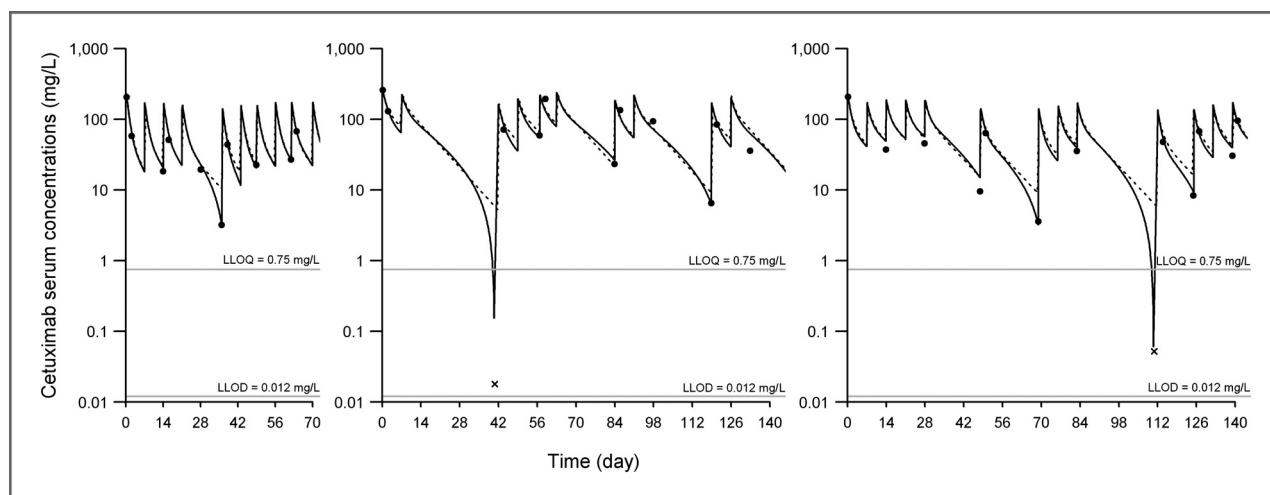


Figure 1. Observed (closed circles) and model-predicted (lines) cetuximab serum concentrations as a function of time in 3 representative patients. Results of the 2 compartment model with only linear elimination or with both linear and nonlinear elimination are displayed as dashed and solid lines, respectively. Initial dose was 400 mg/m<sup>2</sup>, followed by weekly doses of 250 mg/m<sup>2</sup>.

cetuximab infusions 3 months before their progression. Other potential prognostic factors did not significantly influence PFS.

A trend toward improved survival was observed in patients who had experienced cetuximab skin toxicity of any grade within the first 21 days of treatment ( $P = 0.077$ ).

### Discussion

This is the first study analyzing the influence of cetuximab pharmacokinetics on its efficacy in metastatic colorectal

cancer patients. Individual exposure to cetuximab was estimated by a population pharmacokinetic approach, and cetuximab global clearance showed a significant influence on PFS. To our knowledge, the only previous study analyzing the relationship between the serum concentrations of cetuximab and its efficacy was that of Fracasso and colleagues, who observed higher trough concentrations in responders than in nonresponders, in a cohort of patients treated for different types of carcinomas (10).

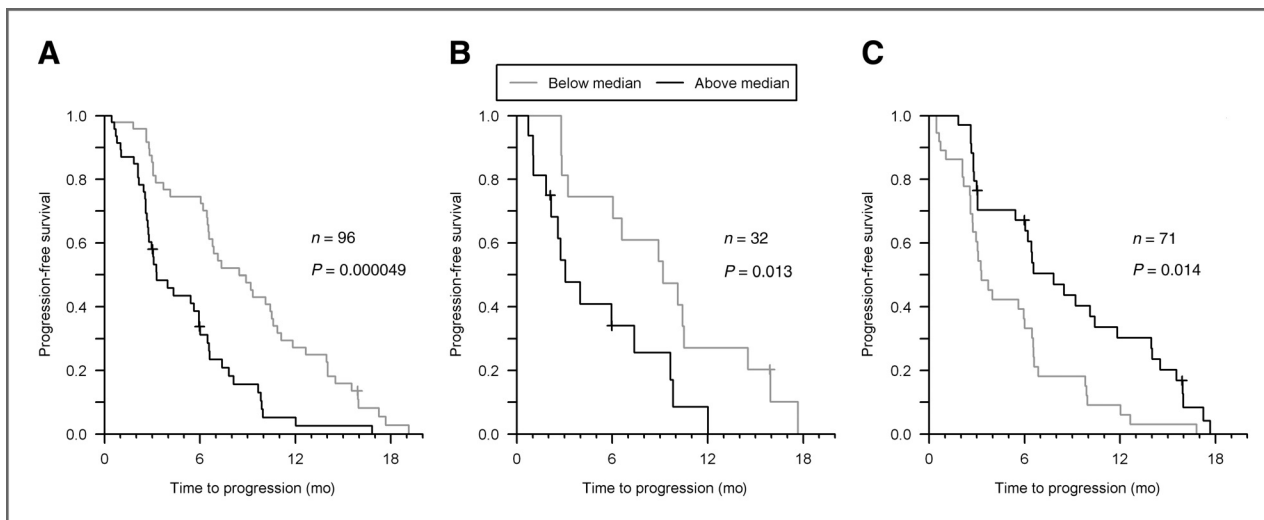
The first population pharmacokinetic study of cetuximab was reported by Dirks and colleagues in head and neck

Table 2. Estimated cetuximab pharmacokinetic parameters

|                                      | Parameter | Standard error | Relative standard error, <sup>a</sup> % | P        |
|--------------------------------------|-----------|----------------|---|----------|
| $V_1$ , L                            | 2.96      | 0.12           | 4                                       |          |
| $CL$ , L/d                           | 0.497     | 0.021          | 4                                       |          |
| $V_2$ , L                            | 4.65      | 0.29           | 6                                       |          |
| $Q$ , L/d                            | 0.836     | 0.07           | 8                                       |          |
| $k_0$ , mg/d                         | 8.71      | 0.84           | 10                                      |          |
| $\beta_{V_1}$ (BSA)                  | 0.42      | 0.17           | 41                                      | 0.015    |
| $\beta_{V_2}$ (BSA)                  | 0.56      | 0.27           | 49                                      | 0.039    |
| $\beta_{V_0}$ (BSA)                  | 1.58      | 0.35           | 22                                      | 0.000078 |
| $\beta_{CL}$ (initial serum albumin) | -0.0244   | 0.009          | 37                                      | 0.0064   |
| $\omega_{V_1}^2$                     | 0.0725    | 0.02           | 28                                      |          |
| $\omega_{CL}^2$                      | 0.11      | 0.018          | 17                                      |          |
| $\omega_{V_2}^2$                     | 0.21      | 0.048          | 23                                      |          |
| $\omega_Q$                           | 0.305     | 0.076          | 25                                      |          |
| $\omega_{k_0}$                       | 0.215     | 0.041          | 19                                      |          |
| $\sigma_{prop}^2$                    | 0.222     | 0.0053         | 2                                       |          |

Abbreviations:  $V_1$  and  $V_2$ , respectively central and peripheral volumes of distribution;  $CL$  and  $Q$ , respectively elimination and distribution clearances;  $k_0$ , zero-order elimination.

<sup>a</sup>(%) Relative standard error: (standard error/parameter value)  $\times$  100.



**Figure 2.** Kaplan–Meier curves of PFS according to (A) cetuximab global clearance in all patients, (B) cetuximab global clearance in patients with wild-type *KRAS* tumor, and (C) cetuximab residual concentration on day 14. Patients with values above and below the median value are displayed as black and gray lines, respectively.

cancer patients (24). The authors described all cetuximab elimination as nonlinear, using a model based on the Michaelis–Menten equation. In the present study, a model combining linear and nonlinear eliminations gave better results, a fact that may be explained by the differences in patient populations (metastatic colorectal cancer vs. head and neck cancer). The superiority of this latter model was more pronounced at cetuximab concentrations lower than 10 mg/L (Fig. 1) when one of the weekly infusions of cetuximab had been omitted.

The elimination of plasma proteins, including IgG and albumin, occurs via intracellular catabolism, following fluid-phase endocytosis, a mechanism that is not saturable (30). A fraction of endocytosed IgG (and albumin) is

protected from degradation by a specific receptor, FcRn, whose function is not saturated at therapeutic concentrations of monoclonal antibodies (30). Antibodies also undergo receptor-mediated elimination after binding to their target antigen. This latter elimination is, by definition, capacity limited (saturable) because of finite availability of the target antigen. The structural model used in the present study should therefore provide a more mechanistic description of cetuximab elimination than the other models tested, because it takes into account the different mechanisms of elimination and combines nonsaturable (first-order) and saturable (zero-order) eliminations. The relationship between early skin toxicity and  $k_0$  but not  $CL$  seems to indicate that the zero-order elimination depicts an EGFR-specific elimination pathway and that the first-order elimination pathway does not. A similar type of model was previously used to describe the pharmacokinetics of panitumumab, another anti-EGFR monoclonal antibody (11), the saturable part of elimination being described by a Michaelis–Menten equation.

Cetuximab pharmacokinetics was also previously analyzed by nonparametric approaches, either given as monotherapy in different types of solid tumors (23) or associated with irinotecan and 5-fluorouracil/folinic acid (FOLFIRI) in metastatic colorectal cancer (25). Tan and colleagues reported a significant association between cetuximab clearance and both BSA and weight (23). We observed an influence of BSA on  $V_1$ ,  $V_2$ , and  $k_0$ , the zero-order constant describing the saturable elimination of cetuximab. The dosing of this monoclonal antibody is indeed based on BSA. The increase in  $k_0$  with BSA may be explained by the fact that EGFR is also present at the surface of normal epidermal cells and that, therefore, target-mediated elimination increases with BSA. We also observed an inverse relationship between initial serum albumin concentration and the nonsaturable component of cetuximab

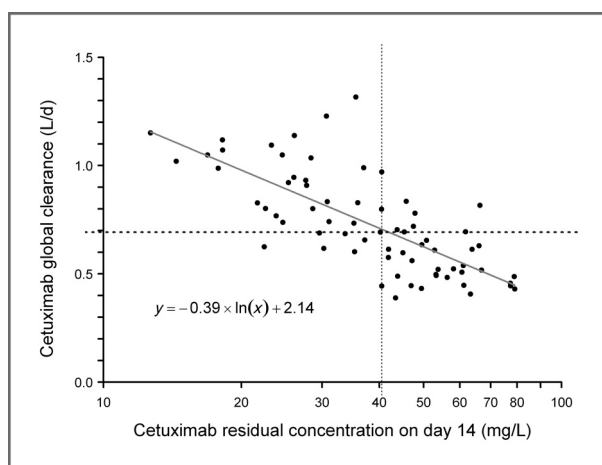


**Figure 3.** Log-linear relationship between cetuximab residual concentration on day 14 ( $x$ ) and cetuximab global clearance ( $y$ ) in 71 patients. Dotted lines correspond to median values of cetuximab global clearance (horizontal) and cetuximab residual concentration on day 14 (vertical).

**Table 3.** Results of Kaplan–Meier and Cox analyses

| Covariate                              | Median (range)   | Kaplan–Meier analysis |        |        |          | Cox analysis |       |                |                 |          |  |
|--|------------------|-----------------------|--------|--------|----------|--------------|-------|----------------|-----------------|----------|--|
|  |                  | Patients              | Events | TTPmed | 95% CI   | Coefficient  | HR    | Standard error | $\Delta^{-2LL}$ | P        |  |
| Global clearance                       | 0.65 (0.27–1.31) | 96                    |        |        |          |              |       |                |                 |          |  |
| Below or equal median value            | 0.49 (0.27–0.65) | 48                    | 43     | 8.48   | 6.6–10.9 | 0            | 1     |                |                 |          |  |
| Above median value                     | 0.83 (0.65–1.31) | 48                    | 43     | 3.29   | 2.8–6.0  | 0.946        | 2.576 | 0.231          | 8.25            | 0.000049 |  |
| Residual concentration at 14 days      | 40.5 (12.7–79.0) | 71                    |        |        |          |              |       |                |                 |          |  |
| Below or equal median value            | 27.8 (12.7–40.5) | 36                    | 32     | 3.71   | 3.0–6.5  | 0            | 1     |                |                 |          |  |
| Above median value                     | 53.2 (41.9–79.0) | 35                    | 32     | 6.57   | 5.4–11.8 | –0.782       | 0.457 | 0.270          | 4.18            | 0.004    |  |
| Global clearance wild-type <i>KRAS</i> | 0.69 (0.33–1.12) | 32                    |        |        |          |              |       |                |                 |          |  |
| Below or equal median value            | 0.49 (0.33–0.69) | 16                    | 14     | 9.20   | 6.0–NA   | 0            | 1     |                |                 |          |  |
| Above median value                     | 0.94 (0.69–1.12) | 16                    | 14     | 3.06   | 2.17–NA  | 1.024        | 2.784 | 0.415          | 3.05            | 0.013    |  |

Abbreviation: TTPmed, median time to progression.

elimination. Such an association was also reported both for bevacizumab (31) and for infliximab (32). Because both albumin and IgG are protected by FcRn (33), their clearance may be affected in similar ways by modifications of FcRn activity.

To study the relationship between cetuximab concentration and clinical response, we used time to progression to construct Kaplan–Meier curves of PFS. The potential influence of time-independent prognostic factors was analyzed by Cox proportional hazards regressions (Table 3). Because the cumulative AUC is dependent on time to progression and time of follow-up, we used cetuximab global clearance (cumulative cetuximab dose divided by cumulative AUC) to obtain a time-independent marker of individual elimination of cetuximab. The risk of disease progression decreased significantly with decreasing cetuximab global clearance. Because the assessment of cetuximab global clearance requires pharmacokinetic modeling that relies on samples taken over time, we investigated whether early cetuximab residual concentration (day 14) could provide a relevant index of patient exposure. Cetuximab trough concentrations on day 14 were a good index of global clearance (Fig. 3) and were significantly related to PFS (Fig. 2C). The present study included an individual dose adjustment of irinotecan and 5-fluorouracil, and our results may not apply to standard dosing regimens. Although the relationship between cetuximab clearance and PFS might be broadly applicable, our results therefore need to be confirmed.

We observed no significant effect of *FCGR3A*-V158F genetic polymorphism on PFS. Bibeau and colleagues studied metastatic colorectal cancer patients treated by cetuximab and observed that *FCGR3A*-158V/V patients had a better response than those carrying the *FCGR3A*-158F allele (34). However, our studies are different in several aspects. In

the present study, all patients were treated by optimized FOLFIRI (5-fluorouracil/folinic acid and irinotecan) whereas 67 of 68 patients of the study of Bibeau and colleagues were cotreated by conventional doses of irinotecan only (34). In addition, in our study, an individual dose optimization was done for irinotecan based on *UGT1A1* genotyping and for 5-fluorouracil based on both DPD (13) and 5-fluorouracil plasma concentration monitoring (14). This individualized and stronger associated chemotherapy may have hidden the effect of *FCGR3A* polymorphism on cetuximab therapeutic effect.

For both cetuximab (2) and panitumumab (35), a correlation between skin toxicity and survival was reported. In the present study, such a relationship was observed but it did not reach statistical significance ( $P = 0.077$ ). This may be explained by the individual dose intensification of irinotecan and 5-fluorouracil carried out: these drugs playing a larger role in patients' response than in conventional chemotherapy regimens used in previous studies.

The *KRAS* status of the tumor, which was available in a subgroup of 51 patients, had no direct significant influence on PFS. Mutation of *KRAS* tumor is, however, a well-established negative predictive factor of response to anti-EGFR monoclonal antibodies (5). The present study was started in 2004, before the influence of *KRAS* status on cetuximab response has been reported (5, 36, 37). As a consequence, tumor tissue was not available for all patients and the lack of a significant influence of *KRAS* status may be explained by an insufficient power of our study. Again, the individual dose intensification of chemotherapy done in the present study may have compensated for the negative effect of *KRAS* mutation on the response to cetuximab. However, *KRAS* status did influence the relationship between cetuximab global clearance and PFS: in the wild-type *KRAS* group but

not in the mutated *KRAS* group, risk of disease progression increased significantly with cetuximab global clearance.

In conclusion, using our sampling times, a 2-compartment model with combined linear and nonlinear eliminations provided the best estimation of cetuximab pharmacokinetics. Cetuximab pharmacokinetics, as assessed by global clearance and by cetuximab concentration on day 14, influences PFS of metastatic colorectal cancer patients treated in association with optimized FOLFIRI. These results strongly indicate that cetuximab dose and dosing regimen should be optimized, based on an individual assessment of its pharmacokinetics, to extend PFS in metastatic colorectal cancer patients. Nevertheless, this hypothesis needs to be confirmed in a prospective study, including only patients with wild-type *KRAS* tumors.

### Disclosure of Potential Conflicts Of Interest

Commercial research support was obtained from Abbott Pharma, Merck Serono, Roche, Janssen, and LFB.

### References

- Jemal A, Murray T, Ward E, Samuels A, Tiwari RC, Ghafoor A, et al. Cancer statistics, 2005. *CA Cancer J Clin* 2005;55:10–30.
- Saltz LB, Meropol NJ, Loehrer PJ Sr, Needle MN, Kopit J, Mayer RJ. Phase II trial of cetuximab in patients with refractory colorectal cancer that expresses the epidermal growth factor receptor. *J Clin Oncol* 2004;22:1201–8.
- Cunningham D, Humblet Y, Siena S, Khayat D, Bleiberg H, Santoro A, et al. Cetuximab monotherapy and cetuximab plus irinotecan in irinotecan-refractory metastatic colorectal cancer. *N Engl J Med* 2004;351:337–45.
- Lenz HJ, Van Cutsem E, Khambata-Ford S, Mayer RJ, Gold P, Stella P, et al. Multicenter phase II and translational study of cetuximab in metastatic colorectal carcinoma refractory to irinotecan, oxaliplatin, and fluoropyrimidines. *J Clin Oncol* 2006;24:4914–21.
- Lievre A, Bachet JB, Le Corre D, Boige V, Landi B, Emile JF, et al. *KRAS* mutation status is predictive of response to cetuximab therapy in colorectal cancer. *Cancer Res* 2006;66:3992–5.
- Benvenuti S, Sartore-Bianchi A, Di Nicolantonio F, Zanon C, Moroni M, Veronese S, et al. Oncogenic activation of the RAS/RAF signaling pathway impairs the response of metastatic colorectal cancers to anti-epidermal growth factor receptor antibody therapies. *Cancer Res* 2007;67:2643–8.
- Di Fiore F, Blanchard F, Charbonnier F, Le Pessot F, Lamy A, Galais MP, et al. Clinical relevance of *KRAS* mutation detection in metastatic colorectal cancer treated by cetuximab plus chemotherapy. *Br J Cancer* 2007;96:1166–9.
- De Roock W, Piessevaux H, De Schutter J, Janssens M, De Hertogh G, Personeni N, et al. *KRAS* wild-type state predicts survival and is associated to early radiological response in metastatic colorectal cancer treated with cetuximab. *Ann Oncol* 2008;19:508–15.
- Qiu LX, Mao C, Zhang J, Zhu XD, Liao RY, Xue K, et al. Predictive and prognostic value of *KRAS* mutations in metastatic colorectal cancer patients treated with cetuximab: A meta-analysis of 22 studies. *Eur J Cancer* 2010;46:2781–7.
- Fracasso PM, Burris H III, Arquette MA, Govindan R, Gao F, Wright LP, et al. A phase I escalating single-dose and weekly fixed-dose study of cetuximab: pharmacokinetic and pharmacodynamic rationale for dosing. *Clin Cancer Res* 2007;13:986–93.
- Ma P, Yang BB, Wang YM, Peterson M, Narayanan A, Sutjandra L, et al. Population pharmacokinetic analysis of panitumumab in patients with advanced solid tumors. *J Clin Pharmacol* 2009;49:1142–56.
- Ternant D, Paintaud G. Pharmacokinetics and concentration-effect relationships of therapeutic monoclonal antibodies and fusion proteins. *Expert Opin Biol Ther* 2005;5 Suppl 1:S37–47.
- Boisdron-Celle M, Remaud G, Traore S, Poirier AL, Gamelin L, Morel A, et al. 5-Fluorouracil-related severe toxicity: a comparison of different methods for the pretherapeutic detection of dihydropyrimidine dehydrogenase deficiency. *Cancer Lett* 2007;249:271–82.
- Gamelin E, Delva R, Jacob J, Merrouche Y, Raoul JL, Pezet D, et al. Individual fluorouracil dose adjustment based on pharmacokinetic follow-up compared with conventional dosage: results of a multicenter randomized trial of patients with metastatic colorectal cancer. *J Clin Oncol* 2008;26:2099–105.
- Gamelin E, Boisdron-Celle M, Delva R, Regimbeau C, Cailleux PE, Alleaume C, et al. Long-term weekly treatment of colorectal metastatic cancer with fluorouracil and leucovorin: results of a multicentric prospective trial of fluorouracil dosage optimization by pharmacokinetic monitoring in 152 patients. *J Clin Oncol* 1998;16:1470–8.
- Rouits E, Boisdron-Celle M, Dumont A, Guerin O, Morel A, Gamelin E. Relevance of different UGT1A1 polymorphisms in irinotecan-induced toxicity: a molecular and clinical study of 75 patients. *Clin Cancer Res* 2004;10:5151–9.
- Dall'Ozzo S, Andres C, Bardos P, Watier H, Thibault G. Rapid single-step FCGR3A genotyping based on SYBR Green I fluorescence in real-time multiplex allele-specific PCR. *J Immunol Methods* 2003;277:185–92.
- Ceze N, Ternant D, Piller F, Degenne D, Azzopardi N, Dorval E, et al. An enzyme-linked immunosorbent assay for therapeutic drug monitoring of cetuximab. *Ther Drug Monit* 2009;31:597–601.
- Lavielle M, Mentre F. Estimation of population pharmacokinetic parameters of saquinavir in HIV patients with the MONOLIX software. *J Pharmacokinetic Pharmacodyn* 2007;34:229–49.
- Panhard X, Samson A. Extension of the SAEM algorithm for nonlinear mixed models with 2 levels of random effects. *Biostatistics* 2009;10:121–35.
- Baselga J, Pfister D, Cooper MR, Cohen R, Burtneis B, Bos M, et al. Phase I studies of anti-epidermal growth factor receptor chimeric antibody C225 alone and in combination with cisplatin. *J Clin Oncol* 2000;18:904–14.
- Robert F, Ezekiel MP, Spencer SA, Meredith RF, Bonner JA, Khazaeli MB, et al. Phase I study of anti-epidermal growth factor receptor

### Acknowledgments

The authors thank the investigators who included patients in the study: Olivier Capitain, Jean-Philippe Metges, Antoine Adenis, Jean-Luc Raoul, You Heng Lam, Roger Faroux, Claude Maslah, and Virginie Berger. We also thank Jean-Christophe Pagès (Department of Biochemistry of Tours) for his logistical help with the samples.

### Grant Support

N. Azzopardi benefited from a PhD grant from *Conseil général d'Indre-et-Loire*. Development of cetuximab ELISA was partly financed by a master grant from Merck-Serono. *FCGR3A* genotyping and measurement of cetuximab serum concentrations were carried out within the CePiBAC platform. CePiBAC is cofinanced by the European Union. Europe is committed to the region Centre with the European Regional Development Fund.

The costs of publication of this article were defrayed in part by the payment of page charges. This article must therefore be hereby marked *advertisement* in accordance with 18 U.S.C. Section 1734 solely to indicate this fact.

Received May 5, 2011; revised July 14, 2011; accepted July 31, 2011; published OnlineFirst September 27, 2011.



- antibody cetuximab in combination with radiation therapy in patients with advanced head and neck cancer. *J Clin Oncol* 2001;19:3234–43.
23. Tan AR, Moore DF, Hidalgo M, Doroshow JH, Poplin EA, Goodin S, et al. Pharmacokinetics of cetuximab after administration of escalating single dosing and weekly fixed dosing in patients with solid tumors. *Clin Cancer Res* 2006;12:6517–22.
  24. Dirks NL, Nolting A, Kovar A, Meibohm B. Population pharmacokinetics of cetuximab in patients with squamous cell carcinoma of the head and neck. *J Clin Pharmacol* 2008;48:267–78.
  25. Taberero J, Ciardiello F, Rivera F, Rodriguez-Braun E, Ramos FJ, Martinelli E, et al. Cetuximab administered once every second week to patients with metastatic colorectal cancer: a two-part pharmacokinetic/pharmacodynamic phase I dose-escalation study. *Ann Oncol* 2010;21:1537–45.
  26. Bonate PL. The effect of collinearity on parameter estimates in non-linear mixed effect models. *Pharm Res* 1999;16:709–17.
  27. Maitre PO, Buhner M, Thomson D, Stanski DR. A three-step approach combining Bayesian regression and NONMEM population analysis: application to midazolam. *J Pharmacokinet Biopharm* 1991;19:377–84.
  28. Webster-Gandy JD, How C, Harrold K. Palmar-plantar erythrodysesthesia (PPE): a literature review with commentary on experience in a cancer centre. *Eur J Oncol Nurs* 2007;11:238–46.
  29. Bergstrand M, Karlsson MO. Handling data below the limit of quantification in mixed effect models. *Aaps J* 2009;11:371–80.
  30. Wang W, Wang EQ, Balthasar JP. Monoclonal antibody pharmacokinetics and pharmacodynamics. *Clin Pharmacol Ther* 2008;84:548–58.
  31. Lu JF, Bruno R, Eppler S, Novotny W, Lum B, Gaudreault J. Clinical pharmacokinetics of bevacizumab in patients with solid tumors. *Cancer Chemother Pharmacol* 2008;62:779–86.
  32. Fasanmade AA, Adedokun OJ, Ford J, Hernandez D, Johanns J, Hu C, et al. Population pharmacokinetic analysis of infliximab in patients with ulcerative colitis. *Eur J Clin Pharmacol* 2009;65:1211–28.
  33. Chaudhury C, Mehnaz S, Robinson JM, Hayton WL, Pearl DK, Roopenian DC, et al. The major histocompatibility complex-related Fc receptor for IgG (FcRn) binds albumin and prolongs its lifespan. *J Exp Med* 2003;197:315–22.
  34. Bibeau F, Lopez-Crapez E, Di Fiore F, Thezenas S, Ychou M, Blanchard F, et al. Impact of Fc $\gamma$ R1IIa-Fc $\gamma$ R1IIa polymorphisms and KRAS mutations on the clinical outcome of patients with metastatic colorectal cancer treated with cetuximab plus irinotecan. *J Clin Oncol* 2009;27:1122–9.
  35. Peeters M, Siena S, Van Cutsem E, Sobrero A, Hendlisz A, Cascinu S, et al. Association of progression-free survival, overall survival, and patient-reported outcomes by skin toxicity and KRAS status in patients receiving panitumumab monotherapy. *Cancer* 2009;115:1544–54.
  36. Amado RG, Wolf M, Peeters M, Van Cutsem E, Siena S, Freeman DJ, et al. Wild-type KRAS is required for panitumumab efficacy in patients with metastatic colorectal cancer. *J Clin Oncol* 2008;26:1626–34.
  37. Van Cutsem E, Kohne CH, Hitre E, Zaluski J, Chang Chien CR, Makhson A, et al. Cetuximab and chemotherapy as initial treatment for metastatic colorectal cancer. *N Engl J Med* 2009;360:1408–17.